Optical and Magnetic Properties of MBE-Grown Manganese Sulfide Layers

W. Heimbrodt* and L. Chen
Department of Physics and Material Sciences Center, Philipps University, Renthof 5, D-35032 Marburg, Germany

H.-A. Krug Von Nidda and A. Loidl
Center for Electronic Correlation and Magnetism, University Augsburg, D-86159 Augsburg, Germany

P. J. Klar
Institute of Experimental Physics I, Justus-Liebig University of Giessen, Heinrich-Buff-Ring 16, D-35392 Giessen, Germany

L. David and K. A. Prior
School of Engineering and Physical Sciences, Heriot-Watt University, Edinburgh EH14 4AS, U.K.

Metastable zinc-blende MnS layers of various thicknesses from 1.8 nm to 8.6 nm have been grown by molecular beam epitaxy on (100) GaAs between ZnSe cladding layers. We studied the dependences of the optical and the magnetic properties on the layer thickness. On the one hand, the non-exponential decay of the Mn internal transition is found to be faster for thicker layer, which is a size effect and not caused by the interfaces. On the other hand, the Néel-temperature is not altered with decreasing layer thickness, but the phase-transition-induced shift of the internal Mn transitions is smaller for thinner MnS layers. This is explained by the dominating influence of Mn ions at the interface, which possess a reduced number of Mn neighbors. SQUID measurements in a weak external magnetic field confirm the optical observations in zero field. However, applying a strong magnetic field reveals the metamagnetic character of these zinc-blende MnS layers. An ntiferromagnetic-to-ferromagnetic phase transition is found with increasing external field.

I. INTRODUCTION

How much the size of a material can be reduced before losing its macroscopic properties is an interesting and important question these days. Regarding electronic correlations and magnetism, the question is still open despite the fact that today's material preparation methods allow one to achieve structure sizes with dimensions where quantum effects dominate. Manganese sulfide in the metastable zinc-blende (ZB) structure is a fcc type-III antiferromagnet, which can be well described by the Heisenberg-type approximation. Ideal two-dimensional systems of a Heisenberg type do not develop any kind of long-range magnetic order down to the lowest temperatures as was rigorously proven by using the spin-wave theory (Mermin-Wagner theorem) [1]. Real magnetic nanostructures usually do not fulfill the assumptions of the theorem due to finite anisotropy. Here, we study the optical and the magnetic properties of MnS layers grown by using molecular beam epitaxy (MBE). Due to the lattice constant of ZB MnS being close to that of both GaAs and ZnSe, we were able to grow layers of controlled thickness. It is the aim of the paper to study the influence of the 3D $\rightarrow$ 2D crossover on the optical as well as the magnetic properties of the MnS layers.

II. EXPERIMENTAL DETAILS

A Vacuum Generator V80H MBE system was used for growing the MnS/ZnSe heterostructures by using Zn, Se and Mn elemental sources and ZnS as a sulphur source [2]. The MnS layers with defined thicknesses of 1.8, 4.3, 6.5 and 8.6 nm, respectively, embedded between ZnSe layers were grown pseudomorphically on GaAs (100) substrates at growth temperatures of 240 – 270 °C. A thin

*E-mail: Wolfram.Heimbrodt@physik.uni-marburg.de

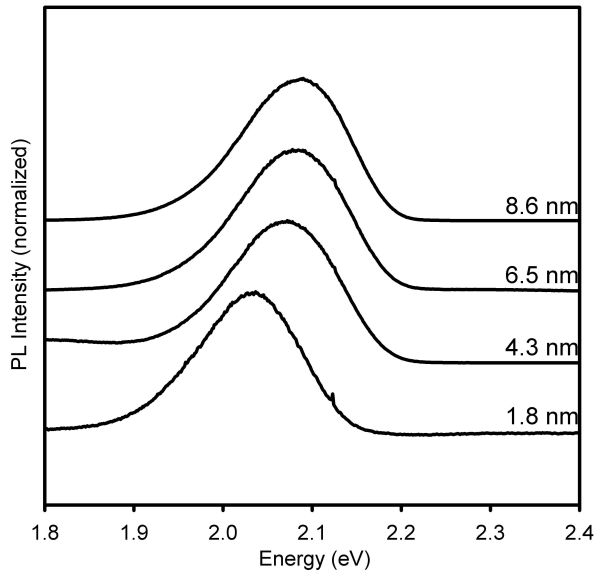

Fig. 1. Normalized PL spectra of MnS layers with different thicknesses at $T = 10$ K.

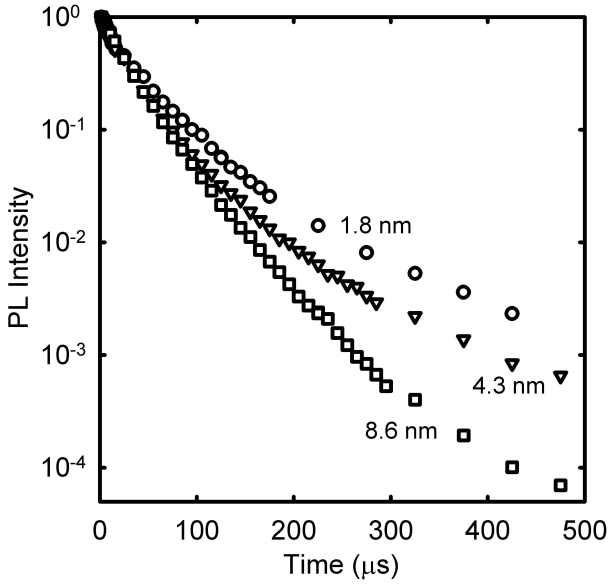

Fig. 2. PL transients of MnS layers with various thicknesses at $T = 10$ K.

(20 – 50 nm) ZnSe buffer layer was deposited prior to the growth of the ZB MnS layer. The MnS was grown using Mn and ZnS sources. Finally, the heterostructure was capped with 20 nm of ZnSe.

Photoluminescence (PL) and time-resolved photoluminescence spectroscopy (TRPL) were performed using a pulsed Nd:YAG laser doubled to 532 nm or tripled to 355 nm. The laser pulse typically has a spectral width of about 5 meV and a duration of about 5 ns. The samples were mounted in a helium cryostat. The PL was focused on to the entrance slit of a 0.25 m grating monochromator and detected by a gated intensified CCD detector system. The PL decay was investigated up to 0.5 ms after the excitation. The maximum temporal resolution was 2 ns. Magnetization measurements were performed in a commercial superconducting quantum interference device (SQUID magnetometer, Quantum design MPMS5) in the temperature range 2 K $\leq T \leq$ 300 K.

III. RESULTS AND DISCUSSION

1. Optical Properties

Figure 1 depicts the PL of MnS for various layer thicknesses at 10 K. The PL is caused by the internal $Mn^{2+}(3d^5)$ transition from the excited state ($^4T_1$) to the ground state ($^6A_1$). The PL position of the 1.8 nm sample is at somewhat smaller energies than that of the thicker layers. We will come back to this point later. In Figure 2 the transients of the PL are depicted for the 1.8 nm, 4.3 nm and 8.6 nm layers. The decay curves are clearly non-exponential, and the characteristic times are much shorter than the intrinsic radiation lifetime for spin and symmetry forbidden transitions. The shortening of the lifetime and the non-exponential decay are caused by the migration of the excitation inside the Mn subsystem and a subsequent transfer to radiationless centers. The thinner layer exhibits a longer lifetime and is a size effect as has been studied in detail recently for Mn-doped ZnS nanostructures [3,4].

Figure 3 depicts the normalized PL bands of the 8.6 nm layer at various temperatures. The PL peak shifts to lower energies with increasing temperature, and its intensity decreases strongly with increasing temperature. Therefore, a very weak PL band at 2.14 eV becomes observable above 100 K. This band is caused by Mn ions in the ZnSe cladding layers and does not show a remarkable shift with temperature. The non-intentionally weak doping of the cladding layers is caused most likely by residual contamination.

In Figure 4, the energy positions are given for the MnS PL as a function of temperature for the 8.6 nm layer compared to the respective PL energies of the 1.8 nm layer. It is obvious that above a critical temperature the maximum of the PL bands does not shift anymore. The total shift for the 1.8 nm layer is about 15 meV, which is about half the shift of the 8.6 nm layer with $\Delta E = 30$ meV. Before we discuss this difference, we have to answer the question, what is the physical reason for the red shift of the Mn PL in the MnS films? It is known from MnS bulk samples [5,6] that below the antiferromagnetic spin ordering temperature, a blue shift of the internal transitions occurs. The physical reason is the energy relaxation of the various $Mn^{2+}(3d^5)$ states due to spin ordering. The maximum shifts of the electronic states between the totally ordered state at $T = 0$ K and the paramagnetic state above the Néel-temperature T_N can

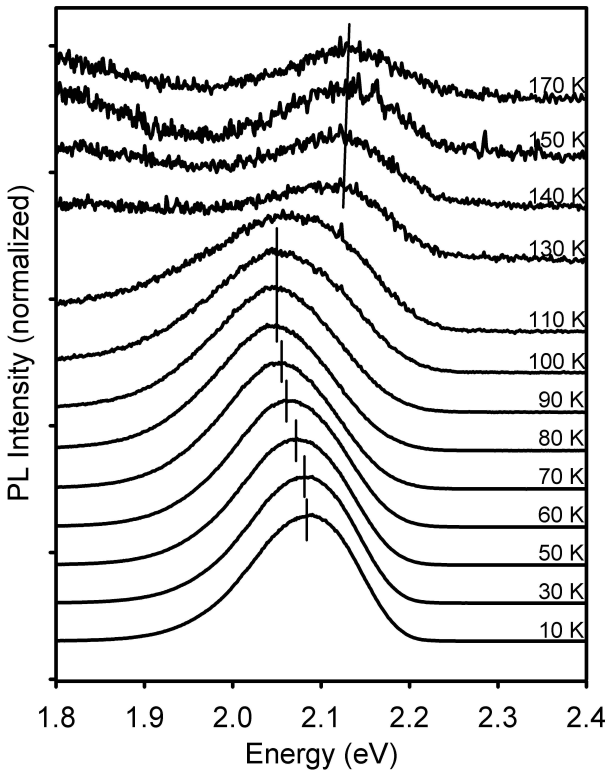

Fig. 3. Normalized PL spectra of the MnS layer with $d = 8.6$ nm at various temperatures.

be estimated in the framework of an isotropic Heisenberg Hamiltonian describing the d-p-d superexchange interaction. Including only the nearest-neighbor (nn) and the next-nearest-neighbor (nnn) interactions, $J_{\rm nn}$ and $J_{\rm nnn}$, respectively, the exchange-interaction-induced relaxation $E(T)$ per Mn ion is obtained in the mean field approximation (MFA) as

$$E(T) = \langle H_{i=1} \rangle = -\sum_j J_{1j} \langle S_1^z \rangle \langle S_j^z \rangle$$

$$= -\langle S_1^z \rangle \left[J_{\rm nn} \sum_{\rm nn} \langle S_1^z \rangle + J_{\rm nnn} \sum_{\rm nnn} \langle S_j^z \rangle \right]. \qquad (1)$$

To apply Eq. (1) to the zinc-blende structure, one has to sum over the given spin-up and spin-down states of the nearest-neighbor and the next-nearest-neighbor shells. For a Mn^{2+} ion in the ground state ($S = 5/2$), this leads to

$$E_g(0) = (4J_{\rm nn} - 2J_{\rm nnn})\, S^2. \qquad (2)$$

At sufficiently low excitation densities, an excited (single) Mn^{2+} ion can be assumed to be placed in an unchanged mean spin-field of neighboring Mn^{2+} ions. For the spin-ordering- induced energy relaxation $E_{ex}(0)$ of such an excited Mn^{2+} ion in one of the lowest-energy (quartet) states ($S^{ex} = 3/2$), one derives

$$E_{ex}(0) = (4J_{\rm nn}^{ex} - 2J_{\rm nnn}^{ex})\, SS^{ex}, \qquad (3)$$

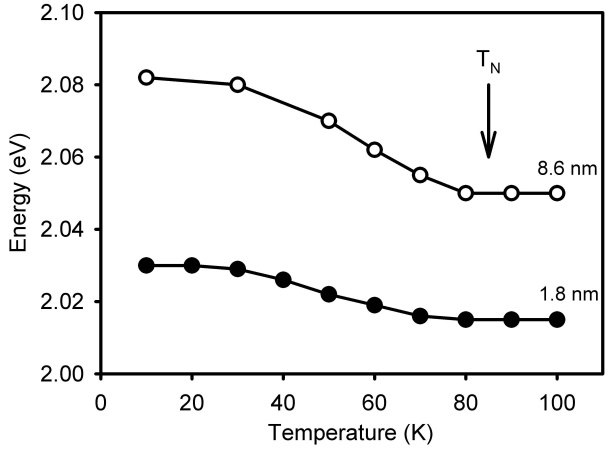

Fig. 4. PL peak position as function of the temperature for MnS layers with different thicknesses.

where $J_{\rm nn}^{ex}$ and $J_{\rm nnn}^{ex}$ denote the exchange interaction parameters between the considered excited Mn^{2+} ion and a nn or nnn Mn^{2+} ion in the ground state. The measured total spin-ordering-induced shift is then given by

$$\triangle E = (E_{ex} - E_g)_{T=0} - (E_{ex} - E_g)_{T_{\rm N}}\,. \qquad (4)$$

In the disordered paramagnetic state above $T_{\rm N}$, no energy relaxation is expected and $(E_{ex} - E_g)_{T_{\rm N}} \equiv 0$. A spin-ordering-induced PL shift results from the different spin quantum numbers $S = 5/2$ and $S^{ex} = 3/2$ of the ground and the excited states. Using experimental values for the ground state exchange integrals, one can estimate the otherwise not accessible exchange interaction parameters for the excited state. Using the known bulk exchange interaction parameter of MnS ($J_{\rm nn}/k = -12.4$ K, $\mid J_{\rm nnn} \mid \ll \mid J_{\rm nn} \mid$ [7]), one can estimate the exchange interaction parameter from the total shift $\Delta E = 30$ meV to $J_{nn}^{ex}/k = +2.05$ K for the $^4T_1$ state of the Mn^{2+} ions in the 8.6 nm layer. The positive value indicates a ferromagnetic spin coupling of the excited state. At a first glance, one might expect smaller exchange integrals for the 1.8 nm sample compared to the thicker sample, resulting in a smaller shift. An important observation is, however, that there is no obvious indication for a decreased Néel-temperature for the thin layer compared to the thick one. The Néel-temperature can be estimated from the low-field SQUID measurements to be about $T_{\rm N} = 85$ K (marked by the arrows in Figure 4 and the dotted line in Figure 5). This value is smaller than the bulk value of zinc-blende MnS which is $T_{\rm N} = 100$ K [8]. This reduced ordering temperature is very likely caused by the biaxial tensile strain. The tetragonal distortion effectively decreases the exchange interaction strength. This is in concordance with observations on MnSe [9] and MnTe [10] layers grown by using MBE. These layers under biaxial compressive strain exhibit an increased Néel-temperature compared to the known bulk values. The same Néel-temperature for the 1.8 nm sample and

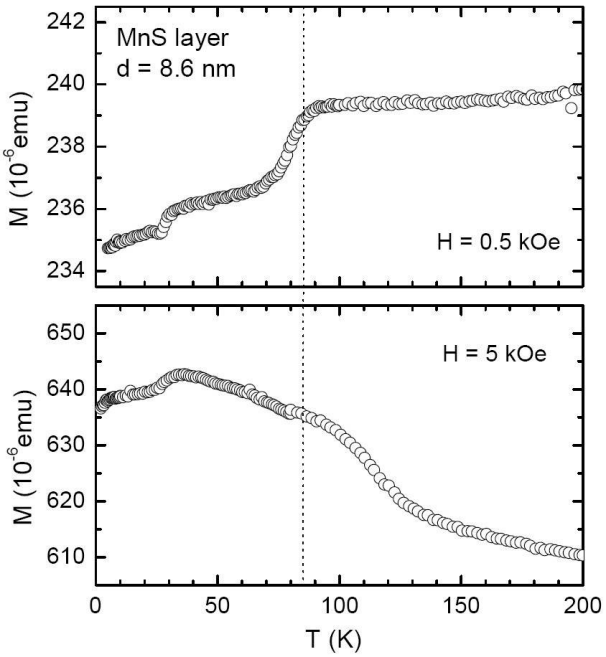

Fig. 5. Temperature dependence of the magnetization for the MnS layer with $d = 8.3$ nm at magnetic fields of 0.5 kOe (upper frame) and 5 kOe (lower frame). The dotted line indicates the Néel temperature $T_N = 85$ K.

for the 8.6 nm sample in Figure 4 indicates that there is no dependence of the exchange interaction parameters on the layer thickness.

How can we explain, then, the clear reduction of the spin ordering induced shift? In what follows, we will show that it is obviously an interface effect. Mn ions at the MnS/ZnSe interface experience a reduced energy relaxation in the spin-ordered state due to the reduced number of Mn neighbors. If a bulk-like fcc type-III antiferromagnetic order is assumed, a manganese ion at an ideal (100) ZnSe/MnS interface would have 5 nn Mn ions with antiparallel spin orientation and 3 nn ions with parallel orientation whereas the nnn shell exhibits two ions with antiparallel spins but 3 ions with parallel spins, yielding for the relaxation energies of the ground and the excited states

$$E_g^{surf}(0) = (2J_{nn} - 1J_{nnn})\, S^2, \tag{5}$$

$$E_{ex}^{surf}(0) = (2J_{nn}^{ex} - 1J_{nnn}^{ex})\, SS^{ex}. \tag{6}$$

Thus, the relaxation energy of the optical transition of a Mn ion at the interface is exactly half of that of a Mn ion in the bulk. Consequently we have to conclude that the Mn ions at the interface dominate in the case of the 1.8 nm layer, yielding a smaller shift, whereas in the 8.6 nm thick layer, the bulk configuration of the Mn ions is still dominant. Actually, more than half of the Mn ions belong to the ultimate or penultimate monolayer in the case of an ideal 1.8 nm MnS layer. Interdiffusion and interface roughness may even enhance the number of Mn ions with a reduced number of nearest neighbors.

It should be noted, that the PL position for the two layers must be different in the spin-ordered state at lowest temperatures. However, it should be the same in the paramagnetic state above the Néel-temperature, but as can be seen in Figure 4, this is not the case. At a first glance, one might expect that this is caused by different crystal fields. As aforementioned, the layers are under tensile strain in case of pseudomorphic growth. Biaxial tensile strain effectively decreases the crystal field, yielding a blue shift of the ${}^4T_1 \rightarrow {}^6A_1$ transition (see *e.g.* [11]. Let us assume that the 8.6 nm layer exceeds already the critical thickness and that a relaxation took place with respective incorporation of dislocations, *etc.* In that case, the crystal field strength would be increased, and a red shift would be expected. This is, however, in contradiction with our observation. At the moment we cannot explain the different energetic positions of the internal $Mn^{2+}(3d^5)$ PL.

2. Magnetism

Further interesting information about the magnetic state of the MnS layers is obtained from the SQUID-measurements. Pieces of a layer with an area of about 6 mm^2 have been measured with the magnetic field applied parallel to the surface of the layer. In Figure 5, the results of the magnetization measurements are depicted for the thick MnS layer as a function of temperature. At low field ($H = 500$ Oe), the magnetization is approximately temperature independent above $T_N = 85$ K, where it decreases on lowering the temperature, as typical for an antiferromagnetic transition, followed by a second weak anomaly. At $H = 5$ kOe, the magnetization surprisingly increases with decreasing temperature below 120 K as for a ferromagnet whereas the transition at T_N remains only weakly discernible. Note that the observed changes of the magnetization are only slightly above the resolution limit of the SQUID magnetometer.

The quasi-ferromagnetic behavior detected at higher magnetic fields is observed in all samples under consideration. The sharpest transition was found in the thin layer with $d = 1.8$ nm, whose magnetization is depicted in Figure 6. Already, at about $2T_N = 170$ K, the onset of a ferromagnetic contribution is observed, and saturation is reached below 100 K.

To verify whether this ferromagnetic contribution really stems from the MnS layer, we estimated the strength of the magnetic moment per Mn spin resulting from the observed increase of the magnetization of 10^{-5} emu in the layer with $d = 1.8$ nm. Using the volume $V = 1.08 \cdot 10^{-8}$ cm^3 of the measured MnS layer and the cubic fcc lattice constant of MnS $a_0 = 5.606$ Å, one obtains about $4.4\mu_B$ per Mn spin, in good agreement with the value of $5\mu_B$ expected for spin $S = 5/2$; *i.e.*, within the

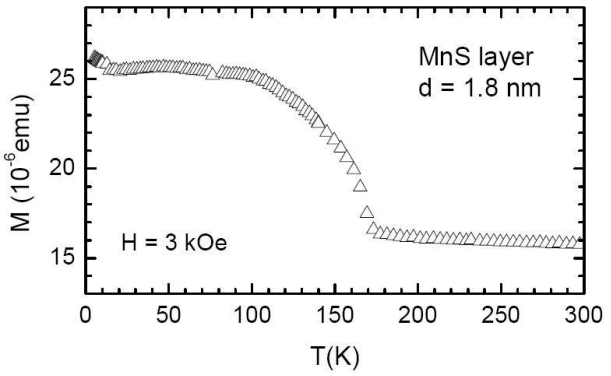

Fig. 6. Temperature dependence of the magnetization for the MnS layer with $d = 1.8$ nm at a magnetic field of 3 kOe.

experimental error, all Mn spins fully contribute to the observed magnetization.

If the origin of the observed ferromagnetism is to be clarified, more detailed magnetization measurements are necessary. So far it seems that the thin MnS-layer feels the strongest constraints due to the surrounding ZnSe layers, giving rise to some kind of metamagnetic transition from the antiferromagnetic phase at zero field to a ferromagnetic phase at magnetic fields of a few kOe.

For $d = 8.3$ nm, the increase in the magnetization is larger than it is for $d = 1.8$ nm because of more spins, but the ferromagnetic moment is not fully developed anymore and even decreases below the anomaly at 30 K. Although the reason for this anomaly, which is visible even at low fields, is not clear at the moment, the reduced moment can be explained as resulting from the competing antiferromagnetic state in bulk MnS.

IV. SUMMARY

In summary, we have demonstrated that the significance of the interface increases with decreasing MnS layer thickness due to the increasing interface-to-volume ratio, leading to considerable changes in the optical and the magnetic properties. However, considering the decay times of the Mn internal transition, the topology, and not so much the interface, is the decisive physical parameter. Regarding the spin ordering effects, we found that the Néel-temperature of the strained layers was smaller than the corresponding bulk value, but it did not depend on layer thickness. The spin-ordering-induced shift of the internal $Mn^{2+}(3d^5)$ PL is, however, much smaller in zero field in the case of the thinnest layer, which is a strong indication for an interface effect, as Mn ions at the interface have a reduced number of Mn neighbors. SQUID measurements reveal a metamagnetic character of the MnS layers. An antiferromagnetic-to-ferromagnetic phase transition is found, which may be caused by the extreme tetragonal distortion and the respective magneto-crystalline anisotropy or by the modified magnetic interactions between Mn ions in the first few interface monolayers due to the reduced number of Mn nearest and next-nearest neighbors. In case of the thinnest layer, all spins are aligned at lowest temperatures whereas in the thick layer, the competing antiferromagnetic coupling reduces the total moment even at higher external magnetic fields.

ACKNOWLEDGMENTS

We are grateful for funding by the German Research Foundation (DFG) in the framework of the priority program SPP 1165 'Nanowires and nanotubes' and via the collaborative research center SFB 484 (Augsburg).

REFERENCES

[1] N. D. Mermin and H. Wagner, Phys. Rev. Lett. **17**, 1133 (1966).
[2] L. David, C. Bradford, X. Tang, T. C. M. Graham, K. A. Prior and B. C. Cavenett, J. Cryst. Growth **251**, 591 (2003).
[3] L. Chen, T. Niebling, D. Stichtenoth, C. Ronning, P. J. Klar and W. Heimbrodt, Phys. Rev. B **76**, 115325 (2007).
[4] L. Chen, F. J. Brieler, W. Heimbrodt, M. Fröba and P. J. Klar, Phys. Rev. B **75**, 241303(R) (2007).
[5] W. Heimbrodt, C. Benecke, O. Goede and H.-E. Gumlich, Phys. Stat. Sol. (b) **154**, 405 (1989).
[6] W. Heimbrodt, O. Goede, I. Tschentscher, V. Weinhold, A. Klimakow, U. Pohl, K. Jacobs and N. Hoffmann, Physica B **185**, 357 (1993).
[7] L. Jansen, R. Ritter and E. Lombardi, Physica **71**, 425 (1974).
[8] J. M. Hastings, L. M. Corliss, W. Kunnmann and D. Mukamel, Phys. Rev. B **24**, 1388 (1981).
[9] N. Samarth, P. Klosowski, H. Luo, T. M. Giebultowicz, J. K. Furdyna, J. J. Rhyne and B. E. Larson, Phys. Rev. B **44**, 4701 (1991).
[10] T. M. Giebultowicz, P. Klosowski, N. Samarth, H. Luo, J. K. Furdyna and J. J. Rhyne, Phys. Rev. B **48**, 12817 (1993).
[11] F. J. Brieler, P. Grundmann, M. Fröba, L. Chen, P. J. Klar, W. Heimbrodt, H.-A. Krug von Nidda, T. Kurz and A. Loidl, Eur. J. Inorg. Chem., 3597 (2005).